ANL-7771

MATERIALS-COOLANT INTERACTIONS RELEVANT TO EBR-II

W. E. Ruther, T. D. Claar,
S. Greenberg, and R. V. Strain

ARGONNE NATIONAL LABORATORY, ARGONNE, ILLINOIS

Printed in the United States of America
Available from
National Technical Information Service
U.S. Department of Commerce
5285 Port Royal Road
Springfield, Virginia 22151
Price: Printed Copy $3.00; Microfiche $0.95

ANL-7771
Reactor Technology

ARGONNE NATIONAL LABORATORY
9700 South Cass Avenue
Argonne, Illinois 60439

MATERIALS-COOLANT INTERACTIONS RELEVANT TO EBR-II

by

W. E Ruther, T. D. Claar,
S. Greenberg, and R. V. Strain

EBR-II Project

April 1971

2

TABLE OF CONTENTS

LIST OF FIGURES

LIST OF FIGURES

LIST OF TABLES

MATERIALS-COOLANT INTERACTIONS RELEVANT TO EBR-II

by

W. E. Ruther, T. D. Claar,
S. Greenberg, and R. V. Strain

ABSTRACT

Investigations of six bellows that had failed in sodium service indicated that sodium penetration of inclusion stringers led to perforation in three of them. Excessive travel of the valve stem was probably the cause of failure of two others. The sixth failure, the only one causing a reactor shutdown, was ascribed to a defect introduced in the manufacturing process.

Investigations of failures in a sodium sampler and in a tool for in-reactor cutting of sensor leads of an instrumented subassembly showed that the presence of sodium was not deleterious.

Type 304L stainless steel fuel cladding and Type 304 stainless steel hexagonal cans exposed to EBR-II primary coolant showed no selective attack or microstructural change that could be attributed to the sodium or to the procedure for postirradiation removal of sodium.

Slow migration of carbon was observed from Type 304 stainless steel foils ($C > 0.04\%$) into Type 304L stainless steel foils ($C < 0.02\%$) immersed in the EBR-II primary sodium. During this experiment, the measured concentration of carbon in the primary sodium varied from 0.4 to 1.3 ppm.

Corrosion of nickel exposed for 380 days to ~920°F primary sodium was 0.08 mg/cm^2.

Deliberately defected mixed-oxide fuel elements exhibited only minor dimensional changes when exposed to 700°F sodium.

In other ex-reactor sodium exposures: (a) free-machining stainless steels were unsuitable for reactor use; (b) modified Belloseal valves were not affected by 5000 cycles in 700°F sodium; (c) brazed joints retained their shear strength in a 2-month test at 850°F; (d) dissolved tin (1500 ppm) in the sodium did not penetrate stainless steel in 1-month tests at 1020 and 1200°F; and (e) nitridation of Type 304 stainless steel was insignificant under simulated conditions of the EBR-II gas/liquid interface.

I. INTRODUCTION

The sodium-cooled Experimental Breeder Reactor II (EBR-II) has recently completed another successful year in its current mission as a fast-flux irradiation facility. Information obtained by members of the EBR-II Project concerning materials-coolant interactions falls within three general categories: (1) examination of special surveillance subassemblies, (2) investigation of components removed from service in the reactor complex, and (3) ex-reactor experiments to pretest materials or equipment before use in the reactor complex. Two reports[1,2] in a continuing series have been issued to describe the results obtained from the two surveillance subassemblies examined to date. A summary report[3] compiled and discussed the data available for the other categories through 1969. The last report is the precursor of this report and provides general information concerning configuration of the EBR-II plant, sodium chemistry, and sodium-removal techniques that will not be repeated here.

Wide ranges of materials, circumstances, and evaluation techniques are involved. For this reason, each investigation is reported as a self-contained unit consisting of the history of the incident, the results of the investigation, and the conclusions.

II. DATA AND RESULTS

A. Analyses of Failures

Only one of the failures to be described caused a reactor shutdown.

Bellows that became perforated while used in non-EBR-II equipment operated by Argonne National Laboratory personnel were examined in an effort to determine common modes of bellows failure. Such information will be useful in preparation of meaningful specifications for bellows-seal valves to be used in reactor-plant modifications.

Failure of a sodium sampler and of a subassembly lead-cutting tool occurred at times when they were not in reactor service and thus did not cause loss of reactor operating time.

1. Bellows from Vent Valve of Secondary Sodium System

In December 1969, leakage of sodium was discovered in vent valve S2-VC-1590 of the reactor's secondary system. Subsequently, the reactor was shut down, and the valve was disassembled for examination. The valve bellows was found to be defective and was sent to ANL-Illinois for a detailed failure analysis.

The valve is a 2-in. offset valve manufactured by the Hammel-Dahl Co. It was installed in the reactor in April 1961 and was first placed in operation in April 1963 (approximate dates). The valve operated at about 770°F at 50-MWt power and was cycled about 400 times before the failure was detected. Its two-ply bellows was fabricated from Type 347 stainless steel foils about 5 mils thick. The dimensions of the bellows, which had a live length of about $1\frac{7}{8}$ in., were about $1\frac{3}{8}$-in. ID x $1\frac{3}{4}$-in. OD. It contained 12 convolutions. The valve was designed for a 1/2-in. stroke; the bellows compressed when the valve was being opened.

The bellows was exposed to secondary sodium on the outside and to air on the inside. The operating pressure was estimated to be about 15 psi.

Visual examination of the bellows (see Fig. 1) revealed a large crack on the outer ply of the second convolution from the end of the bellows nearest the ball. The crack was at the exact spot where the outer ply had been formed over the resistance-welded seam of the inner ply. The outer ply was plastically deformed in this area during fabrication. Figure 2 shows a magnified view of the crack.

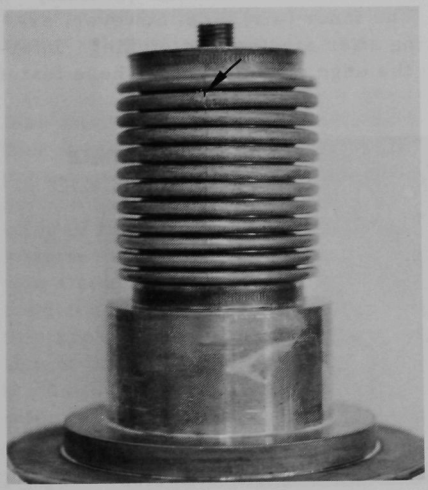

Fig. 1. Bellows from Vent Valve S2-VC-1590 of Secondary System, Showing Large Crack Responsible for Sodium Leak. Mag. ~0.85X. Neg. No. MSD-52562.

Fig. 2. Magnified View, from Sodium Side, of Crack in Bellows from Vent Valve S2-VC-1590. Mag. ~13X. Neg. No. MSD-52563.

The inner bellows ply near the region of the crack exhibited extreme brittleness and deterioration. The inner ply had been completely destroyed in several regions (see Fig. 3).

Fig. 3

Inside (Air Side) of Bellows from Vent Valve S2-VC-1590 in Vicinity of Large Crack, Showing Deterioration and Tearing of Inner Ply. Mag. ~13X. Neg. No. MSD-52564.

After the large crack was filled with a sealant, the bellows was checked on a helium leak detector and by a fluorescent-dye penetrant technique. No additional perforations were discovered.

A metallographic section was taken through the crack in the outer ply by grinding along the axis of the bellows. The outer (sodium) surface showed essentially no attack. The inner (air) side, however, exhibited intergranular attack and cracking after electrolytic etching. Intergranular attack was also evident along the edge of the crack. These features can be seen in Fig. 4.

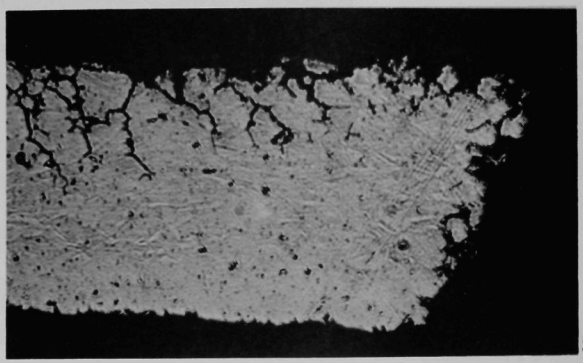

Fig. 4. Transverse Section through Large Crack in Outer Bellows Ply of Vent Valve S2-VC-1590, Showing Intergranular Attack. Inner ply has been completely destroyed in this region. (10-sec etch in 5% oxalic acid). Mag. 250X.

A section of the inner bellows ply from the vicinity of the large crack was also examined. Although the inside (air) surface of this inner ply showed considerable thinning and intergranular penetration, visual examination showed that degradation of the inner ply was confined to the region of the crack.

The metallographic evidence suggests that a small perforation originated in the outer (sodium) ply because of defective bellows material or local stress concentrations. Large localized stresses could have been caused by the plastic deformation introduced into the outer-ply material either when it was formed over the weld seam of the inner ply or possibly during its service lifetime. The bellows was deformed 1/2 in. lengthwise in service, or about 27% of its free length. A 20% maximum deformation is a typical value suggested by manufacturers for a bellows of this type. Thus, the actual deformation was about 135% of that suggested. The bellows operated at about 15 psi, which is roughly 10% of its rated capability. When these values are used on the bellows-lifetime nomograph supplied by a bellows manufacturer,[4] a projected life of about 8000 cycles may be expected. Although this nomograph was derived from room-temperature data, exposure of 770°F would not be expected to significantly decrease the life of a stainless steel bellows.

Further, interpolation of data for bellows life versus flexure obtained by Smith and Whitham[5] for NaK at 482°F leads to a projected lifetime of about 10,000 cycles.

Thus, it seems unlikely that the stresses encountered during service led to the premature failure of the vent-valve bellows, which had been cycled only about 400 times.

Since no evidence was found to indicate that interaction of stainless steel with the EBR-II secondary sodium was responsible for the initiation of the leak, it is postulated that a defect in the outer (sodium) ply was present as a result of the manufacturing process. This initial leak allowed sodium to interact with the small amount of air contained between the two plies of the bellows. The resulting increase in oxygen concentration in the sodium in this isolated region would account for the grain-boundary oxidation along the edge of the crack. The sodium of increased oxygen concentration caused intergranular penetration and embrittlement of both plies in this area. The embrittled inner ply then failed during a subsequent operation of the valve, thereby allowing sodium to gain access to more air inside the bellows body. As the sodium increased again in oxygen concentration, intergranular cracking and extreme deterioration of the inner ply occurred.

2. Bellows from Drain Valve on Core Component Test Loop

On June 5, 1970, failure of a Crane Company 2-in. bellows seal valve on drain line No. 3 of the Core Component Test Loop (CCTL) was detected. The CCTL is operated by the Engineering Technology Division of Argonne National Laboratory. The bellows from this valve was investigated to obtain additional information concerning modes of bellows failure.

The bellows, a convolute-type, single ply bellows with welded seam, was fabricated from Type 347 stainless steel foil 4 mils thick. Its approximate dimensions were $1\frac{1}{2}$-in. OD x $1\frac{1}{8}$-in. ID x 11 in. long. It had been exposed to 600°F (maximum) sodium at 45 psig for 5067 hr and to 665°F (maximum) sodium at 59 psig for 444 hr. CCTL operating records indicate that the bellows had experienced less than 25 open-close cycles as part of the drain-fill operation. The total bellows deflection was about 20% of the live length. Most of the valve's lifetime was spent in the "closed" position. The bellows itself was exposed to liquid sodium on the outside and contained air on the inside.

Fig. 5. Bellows Removed from Drain-line Valve of CCTL. Mag. 1/4X.

Figure 5 shows a photograph of the failed bellows removed from the valve. The major leak site was easily located by visual examination, since the metal in this area appeared to have undergone cracking and tearing. Several small pinhole defects were also in the same convolution as the major defect, and 10 other random pinholes or small cracks were found throughout the bellows by the fluorescent-dye penetrant technique.

Numerous superficial scratches were on the outer surface of the bellows, but the bright metallic luster of the convolutions indicated that the stainless steel had not been oxidized by the sodium. The inner metallic surface of the bellows at the major defect was a dull gray-white. This appearance was in contrast with the darker temper film that was typical of the inner surface of the bellows. Further examination showed the other defect areas detected by the fluorescent-penetrant test to have the same gray-white appearance as the major defect site.

Microscopic study of the specimens from the defect areas showed that the inner surface (air side) of the bellows had been corroded extensively, with the loss of surface grains (see Fig. 6), while the outer

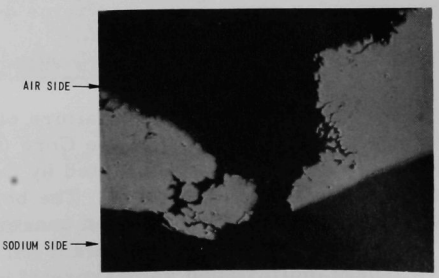

Fig. 6

Section through a Defect Site of Bellows from CCTL Drain-line Valve, Showing Corrosive Attack on Air Side (as polished). Mag. 275X.

surface (sodium side) exhibited no such damage. One weld area exhibited considerable shrinkage. However, neither this weld nor any of the others examined showed any evidence of cracking.

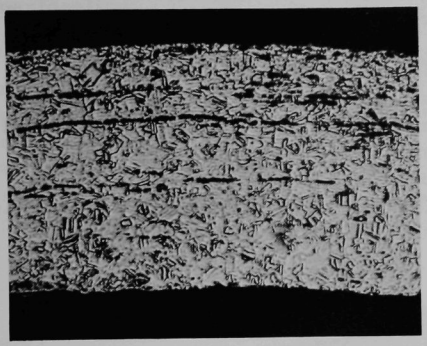

Fig. 7. Typical Network of Nonmetallic Inclusion Stringers in Bellows from CCTL Drain-line Valve (10-sec etch in 5% oxalic acid). Mag. 375X.

The most striking aspect of the microstructure of the stainless steel was the considerable quantity of nonmetallic inclusions present in the material. The inclusions were in the form of long stringers rather than of discrete particles and were in greater abundance than is typical of stainless steel of good quality. The morphology, size, and quantity of inclusions in a typical transverse bellows section can be seen in Fig. 7. These inclusions were apparent in all sections of the bellows examined--not just in isolated areas.

An attempt was made to determine the distribution of the inclusions by placing strips of X-ray film on the outer surface and positioning a radiation source inside the bellows. The radiographs made this way (only alternate convolutions are actually in focus) revealed the defects previously detected by the fluorescent-penetrant test, but provided considerably more resolution of the defects and the surrounding metal.

The most interesting feature of the radiographs was the presence of image lines running circumferentially along the convolutions, as shown in Fig. 8. All convolutions radiographed showed the same general features,

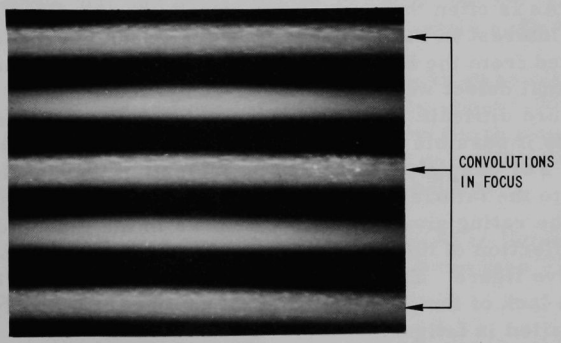

Fig. 8. Magnified Print of X-ray Radiograph of Bellows from CCTL Drain-line Valve, Showing Image Lines of Inclusion Stringers. Mag. 5.25X.

but in some areas the lines formed heavier networks or clusters. This effect was especially apparent adjacent to the previously noted defect sites. In addition to the clustering effect in these regions, dot-like images were noted, which suggests that the features of the metal responsible for the images were also oriented axially in certain areas.

Comparison of the results of radiography and metallography suggested that the nonmetallic inclusions in the stainless steel produced the X-ray images. The image lines and inclusion stringers were oriented in the same direction and had approximately the same size and frequency of appearance. Also, both the inclusions and the images were found generally throughout the bellows. A similar stainless steel bellows containing few, if any, inclusion stringers did not produce any linear or network images when radiographed (see Fig. 9).

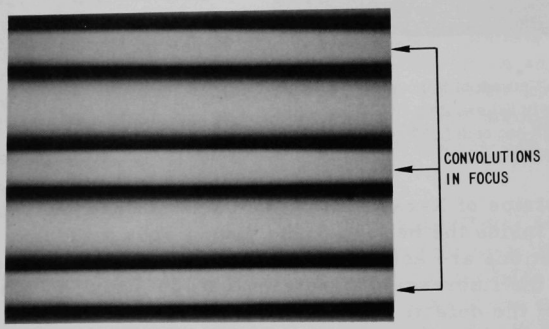

Fig. 9. Magnified Print of an X-ray Radiograph of Bellows with a Clean Microstructure. Note absence of image lines of inclusion stringers. Mag. 5.25X.

As is often the case in investigations of bellows failures, the material of interest in the failure regions had been corroded or mechanically removed from the bellows. Hence, only material somewhat removed from the actual defect was available for study, thus making isolation of mode of failure difficult. However, the evidence accumulated in the investigation made it possible to eliminate several factors with some degree of confidence. For example, there was no indication that mechanical damage contributed to the failure. The pressure across the bellows was only a fraction of the rating given a similar bellows in the manufacturer's catalog. The total deflection of the bellows was of the order of 20% of its live length, a conservative figure. The low number of cycles experienced by the bellows and the lack of incipient fatigue cracks made it unlikely that the component failed in fatigue.

Metallographic studies revealed no evidence of corrosive attack of the liquid sodium on the exposed metal surface of the bellows.

Extensive attack of the air side of the bellows by a mixture of sodium and sodium oxide was noted at the defect sites. However, this is a common observation in failures of this sort and is believed to occur after the initial perforation.

Although the mode of failure could not be conclusively determined, stringers of inclusions appear to have played an active role. Radiographs showed the inclusions to be especially predominant near some of the defect sites. If, as the radiographs suggested, the inclusions were normal to the surface in some areas, sodium could have penetrated along the stringers and dissolved out the inclusions. Eventually, complete sodium penetration of the thin bellows would occur.

3. Bellows from Flowmeter Calibration Equipment

This calibration equipment was operated intermittently for several years by the Engineering Technology Division and then disassembled for moving to another location. The 1-in. Crane valves on the equipment were cleaned and helium leakchecked before the equipment was reassembled. Although no leak had been noted in service, the leakchecks showed that two bellows had perforated enough to give an indication on the helium detector.

One of the bellows had been exposed to argon and sodium vapor for about 600 hr at 300-350°F. The other had been exposed to liquid sodium for about 400 hr at 800-900°F and for about 200 hr at 1000°F.

Both bellows were bright with a metallic luster, and no visual evidence of the leaks was found. The helium leak detector was required to identify the defective areas. In an attempt to pinpoint the leaks, the sections around them were cut out, and dye penetrant was put on one side of the bellows and the developer on the other. With this technique, no leak could be found in the bellows that had been exposed to vapor, but the failure point was identified in the bellows that had been exposed to liquid sodium.

Transverse sections containing the leaks were taken from both bellows and were mounted and ground mechanically, about 0.005 in. at a time, in an effort to find the leakage paths. The 600-grit finish was metallographically polished whenever a suspicious area turned up. No positive identification of the leakage path could be made for either bellows.

The suspect area for the bellows exposed to liquid sodium did show an unusual density of inclusions in stringer form (see Fig. 10) and possible microporosity.

Electroetching with oxalic acid indicated that neither bellows had been held at a high enough temperature at the leak areas to sensitize the stainless steel. Slight penetrations (~1/50 of the total width) into the

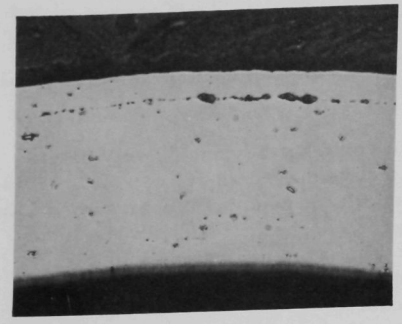

Fig. 10. Inclusion Stringers in Suspect Region of Bellows Exposed to Sodium in Flowmeter Calibration Equipment (as polished). Mag 325X.

bellows wall were noted for both bellows in the etched condition. The penetrations appeared to be associated with grain boundaries, but were never a full grain deep. The penetrations were on the sodium-exposed side of the bellows.

There seemed to be little evidence relating sodium to the small leaks for either bellows. No obvious attack was found. The probable cause of failure was the presence of inclusion stringers in the bellows metal. It is speculated that the sodium penetrated along the stringer, but formed a solid reaction product that was subsequently leached out in the cleaning step. The amount of inclusions in the metal suggested that quality control of the initial bellows stock was poor.

4. Bellows from Life-test Valves

Two Powell Belloseal 2-in. valves cycled in liquid-sodium service by Smith and Jaross of the ANL Engineering Technology Division in two separate series of experiments failed prematurely, one at 1000°F and the other at 1200°F. The results were significant to the EBR-II Project in that valves from the same manufacturer had been purchased for use in a plant modification. The bellows had three plies, each about 10 mils thick, and 12 convolutions. The approximate bellows dimensions were $1\frac{3}{8}$-in. ID x $1\frac{13}{16}$-in. OD x $2\frac{3}{16}$ in. long.

Metallographic examination showed that both bellows failed in a similar manner. Examination by fluorescent-penetrant techniques showed each bellows to have multiple failure sites.

The metal was sensitized, as would be expected from its thermal history. The cracks were long and obvious in the region of the major failures. Major cracks were located in the 180° returns of both bellows, as shown in Fig. 11. The cracks in the bellows tested at 1200°F were all intergranular, as were most of the cracks in the bellows tested at 1000°F. The difference in temperatures of exposure was assumed to be largely responsible for the slight difference in mode of cracking. The multiple cracking in the highly stressed portions of the bellows was similar to the intergranular separations noted in high-temperature creep specimens.

No retained corrosion product was seen in the intergranular penetrations, although the surface exposed to sodium in the bellows tested at 1200°F did have a very thin corrosion coating in the unetched condition

Fig. 11. Crack through Middle Ply of Bellows Valve Life-tested at 1200°F, Showing Intergranular Separation (10-sec etch in 5% oxalic acid). Mag. 350X.

The stem movement on a similar, undamaged valve was 7/8 in., which resulted in a travel of about 40% of the free length of the bellows. This is considerably greater than the usual travel for other bellows valves we have examined. The manufacturer's representative indicated that the bellows was mounted so it was extended about 15% in full-closed position and compressed 25% in the full-open position. In our opinion, this unusually large travel was the primary cause of failure in these bellows. Additional information on this subject is discussed in Sec. II.C.5 of this report.

5. Overheated Primary-sodium Sampler

On August 6, 1969, the heater circuits on the EBR-II primary-sodium sampler were found to be energized while a sample was not being taken. Apparently, the heaters had been left on inadvertently after a sampling operation on August 1, 1969, thereby causing the sampler to overheat.

The tubing carrying the sodium to the sampler was not physically damaged. This was not unexpected, since the temperature of the tubing had not exceeded 800°F. Since the sampler vessel was heated above 1000°F (the upper limit of the temperature indicator), it was removed from the system for examination. Three items were examined: Type 316 stainless steel Swagelok fitting directly connected to the sampler chamber, a section of Type 304 stainless steel tubing, and a section of the Type 304L stainless steel sodium-level probe from the overflow sampler.

Visual observation of the parts made of Types 316 and 304 stainless steel revealed a dark oxide film on the outer surfaces exposed to air. This was not unexpected in view of the high temperature experienced by the sampler. All three components from the sampler then were examined metallographically.

In the as-polished condition, a thick oxide coating was present at the outer surface (air side) of the Type 316 stainless steel Swagelok fitting; below this oxide, a subsurface reaction layer was also found. Etching with oxalic acid revealed that this layer contained nitride precipitates (see Fig. 12); they were similar to the nitrides formed in Type 304 stainless steel foils during exposure to nitrogen at 1020°F for 1 week.

Fig. 12. Type 316 Stainless Steel Swagelok Fitting from Overheated Sodium Sampler (5-sec etch in oxalic acid). Mag. 750X. Neg. No. MSD-51996.

The inner surface, which was exposed to 400-600°F sodium during sampling, also contained a reaction layer. The surface appeared to have undergone nitridation and oxidation, although the oxidation effect was masked by the heavy nitrides present in the layer.

Since the sampler was heated above 1000°F, an effort was made to determine if that temperature was high enough to cause nucleation of sigma phase in the Type 316 stainless steel matrix. Etching of the fitting in boiling potassium ferricyanide solution revealed no sigma-phase particles. This indicated that the overheating was not severe enough to cause formation of the brittle phase, which has been found to form and grow into large precipitates after 1 week at 1650°F.

Carbide precipitates at the grain boundaries indicated that the fitting did reach a temperature within the sensitization range of 1000-1650°F, but the absence of sigma phase suggested that the maximum temperature was less than 1650°F.

The outer surface of the Type 304 stainless steel tubing had a heavier oxide scale than that on the Type 316 stainless steel fitting. The atmospheric oxidation of the tubing penetrated intergranularly to a depth of ~0.8 mil in some areas. The inner surface suffered some degree of intergranular oxidation and some loss of grains. The maximum depth of penetration at the inner surface was less than 1 mil. As in the Type 316 stainless steel fitting, carbide precipitation at the grain boundaries had occurred during sensitization.

The surface appearance along the length of the Type 304L stainless steel level-detector probe indicated that it had been immersed in sodium to a depth of about 1/2 in. during the overheating period. The portion that had been immersed was heavily oxidized to a depth of 1 mil (see Fig. 13). The section that had been in the argon space above the sodium exhibited slight intergranular oxidation less than 0.1 mil deep in isolated areas (see Fig. 14).

The presence of nitrides and oxides in sections exposed to the sodium suggested that air probably entered during the period of overheating. However, not enough information is available to determine how and where such a leak may have developed.

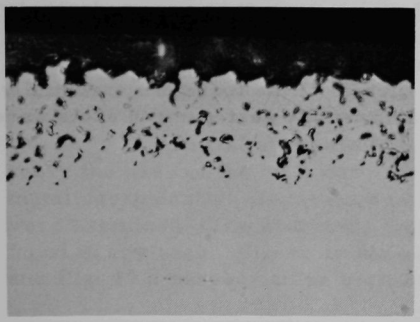

Fig. 13. Portion of Type 304L Stainless Steel Level-detector Probe Exposed to Sodium (as polished). Mag. 750X. Neg. No. MSD-52000.

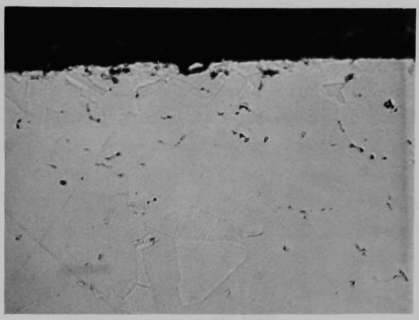

Fig. 14. Portion of Type 304L Stainless Steel Level-detector Probe Exposed to Argon above Sodium (as polished). Mag. 750X. Neg. No. MSD-52001.

Since all interactions on both the air and sodium sides of the sampler components were limited to a depth of about 1 mil, the effects are not expected to be detrimental to the sampler and its operation. The Swagelok fitting, level probe, and tubing have been replaced, and the sampler is functioning satisfactorily.

6. Lead-cutting Tool for Instrumented Subassemblies

A special cutting tool was designed for severing the sensor leads and tubing of instrumented subassemblies before the subassemblies are removed from the reactor. The tool was fabricated of tungsten-bearing high-speed tool steel (Rex AA-AISI T1) of the following nominal composition (in weight percent): W--18.00; C--0.75; Mn--0.30; Si--0.30; Cr--4.00; V--1.15; Fe--balance. The cutting surface was heat-treated to 58-60 Rockwell C, and the hardness of the support cylinder was graded over a $7\frac{1}{2}$-in. length to 35-40 Rockwell C.

The tool performed satisfactorily in the reactor and was stored after use with residual sodium on its surface. On subsequent mechanical testing, the cylinder shattered (see Fig. 15) at substantially less than design torque, although the cutting ears remained intact. In a previous test before their use in the reactor, the tool and its support rod had accidentally impacted on a stainless steel upper adapter fixture. Examination by other investigators at that time did not disclose any damage to the tool.

The tool was examined to determine the cause of failure and, in particular, to determine if corrosion contributed to the failure.

Figure 16 shows an end view of the pieced-together tool. An oblique view (Fig. 17) illustrates one smear of metal on the interior of the

cylinder, which resulted from the accidental impact on an upper adapter fixture. Note that one crack goes through the smear. An analysis of the surface of the metal smear indicated that the smear was stainless steel. The fracture surfaces and the exterior surface of the tool were essentially free of corrosion product, although occasional tiny rust-colored spots were on the fracture surface.

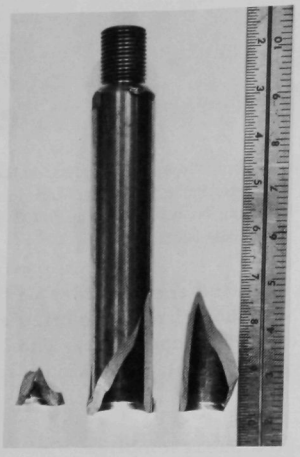

Fig. 15. Shattered Cylinder of Lead-cutting Tool for Instrumented Subassemblies

Fig. 16. End View of Pieced-together Lead-cutting Tool

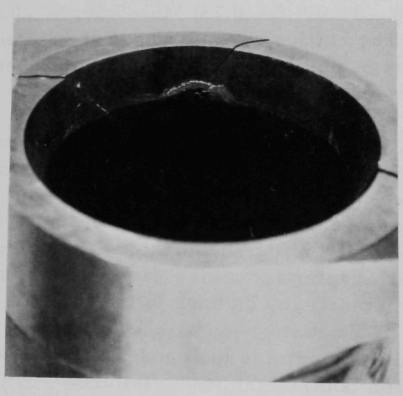

Fig. 17

Oblique View of Lead-cutting Tool, Showing Smeared Metal inside Cylinder

Besides the cracks at which fractures actually occurred, an additional axial crack extending ~$1\frac{1}{8}$ in. up from the base of the tool was

visible to the unaided eye. X-ray examination at a head-on (0°) angle showed this crack. It was not shown, however, by X-ray examination if the beam was at 20° or greater. Magnaflux inspection did not reveal the presence of any additional cracks.

Material at the tip of the large V-shaped fracture (about $2\frac{5}{8}$ in. above the base of the tool) and at the tip of the axial crack was examined metallographically. Sections parallel to, and perpendicular to, the tool axis were examined. The branching typical of stress-corrosion cracks was not found in any case. Figure 18 shows a longitudinal view of the axial crack, and Fig. 19 a perpendicular section at the base of the crack.

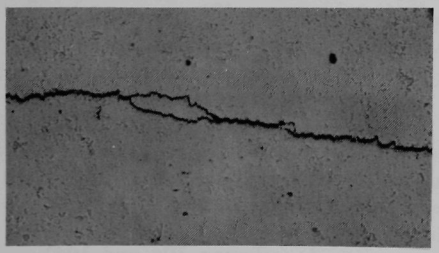

Fig. 18. Longitudinal View of Axial Crack in Cylinder of Lead-cutting Tool (as polished). Mag. 75X.

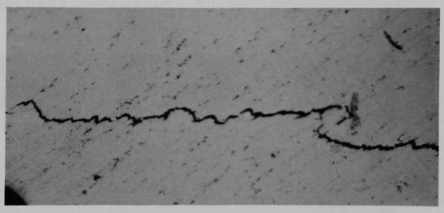

Fig. 19. Perpendicular Section at Base of Axial Crack in Cylinder of Lead-cutting Tool (as polished). Mag. 75X.

If moist-air corrosion of the sodium remaining on the tool during storage had caused hydrogen embrittlement of the high-strength steel, the residual hydrogen content of the metal near the crack should have been substantially greater than normal. A section of metal (~10 x 4 x 2 mm, containing the crack surface) at the base of the axial crack was analyzed for hydrogen. A similar section from the threaded end of the tool was also analyzed. Both samples were cleaned before analysis to remove any surface water (e.g., any water absorbed in the corrosion product at the crack surface). The hydrogen concentrations were:

Vicinity of crack surface	1.3 ppm
Thread end	2.1 ppm

Obviously, no hydrogen had accumulated.

The nature of the crack, the low hydrogen level, and the known previous accident of sufficient force to smear metal all suggest that the tool shattered as a result of physical damage unrelated to corrosion processes.

B. Examination of Materials Exposed to EBR-II Primary Coolant

No reactor components other than driver and experimental-irradiation subassemblies were available for examination the past year.

1. Type 304L Stainless Steel Fuel-element Cladding

Metallographic examination of samples of fuel-element cladding to determine the effects of the reactor primary sodium and the sodium-removal operation on Type 304L stainless steel continued throughout the year. Samples of Mark-IA driver fuel elements having fluences up to 3.5×10^{22} nvt and of Mark-II driver fuel elements having fluences up to 3.3×10^{22} nvt have been examined. For at least some of their total residence in the reactor, the elements were irradiated at higher temperatures (i.e., 1080°F maximum) than in the past, because of the increase in the operating power of the reactor from 50 to 62.5 MWt. As reported previously,[3] the cladding became sensitized in the higher-temperature regions of the element, but showed no evidence of selective attack by the sodium environment or of any microstructural changes that could be attributed to the reactor environment or the sodium-removal procedure. Figure 20 shows a typical microstructure of element cladding that had been irradiated at a calculated temperature of 1065°F.

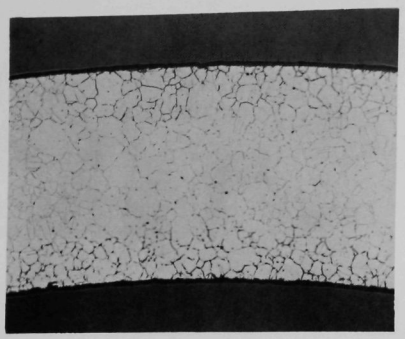

Fig. 20. Cladding from Element 26, from Subassembly B-3079, Exposed at a Calculated Temperature of 1065°F (etched in 10% oxalic acid). Mag. 175X.

2. Types 304 and 304L Stainless Steel Equilibration Foils

Carburization of stainless steels in sodium and the migration of carbon from one alloy to another through liquid sodium have been studied extensively in ex-reactor experiments.[6,7] Although EBR-II reactor components have been examined by metallography and by microprobe and chemical analysis to determine carburization and decarburization effects, no quantitative data have been available as to the carburization potential of primary sodium for stainless steel. As a first step in evaluating this potential, a series of 10-mil-thick stainless steel foils with carbon concentrations ranging from 0.009 to 0.070 wt % was exposed to EBR-II outlet sodium near the exit of a modified driver fuel assembly, B-3074S. The foils were prepared by arc-melting mixtures of commercial Types 304 and 304L stainless steel to give the desired carbon levels. The levels of the major constituents were essentially the same in all melts. Strips of the foil were exposed in a flow-through capsule while controls were exposed in a sealed helium-filled capsule adjacent to the other specimens.

Subassembly B-3074S was in reactor position 6C4 from the start of EBR-II run 37 (August 2, 1969) to the end of run 41B (April 8, 1970)

for a total of 119 days at 50 MWt. Table I shows the history of temperatures and exposure. During the exposure period, several carbon analyses of the sodium were made by the oxyacidic flux method.[8] Table II gives the results of these analyses.

TABLE I. Exposure Histories of Types 304 and 304L Stainless Steel Equilibration Foils

EBR-II Run No.	Outlet Sodium Temp, °F (calculated by HECTIC code)	Cumulative, MWd
37	872	1196
38B	867	1796
39	889	3167
40	888	4534
41	889	5652[a]

Total foil fluence $\cong 2 \times 10^{20}$ nvt (E > 0.1 MeV).

[a]Equivalent to 113 effective full-power days.

TABLE II. Carbon Concentration in Primary Sodium While Stainless Steel Equilibration Foils Were in Reactor

Date	Carbon Concentration, ppm
8/12/69	1.3
9/8/69	0.9
10/30/69	0.4
11/19/69	0.6
1/16/70	0.7
3/26/70	1.1

After the exposure period, the foils were reweighed and analyzed for carbon. Table III shows the initial and final carbon contents and the weight loss of the samples exposed to the sodium. A trend toward a final carbon content of about 0.04% is indicated.

TABLE III. Changes in Carbon Content and Weight of Types 304 and 304L Stainless Steel Equilibration Foils

Foil	Initial Carbon, wt %	Final Carbon, wt %	Measured Weight Loss, mg/cm^2
TC02	0.010	0.036	0.05
TC03	0.018	0.029	0.05
TC05	0.032	0.035	0.03
TC06	0.041	0.042	0.03
TC07	0.048	0.041	0.04
TC08	0.070	0.054	0.02

The nonhomogeneous microstructure (Fig. 21) of the foils whose carbon content had increased indicated that the 0.04 wt % was not an equilibrium value. However, the equilibrium value is apparently between 0.036 and 0.054 wt %. Calculations using diffusivity data of Agarwala et al.[9] indicated a diffusion zone of only 0.00125 in. should be expected on each side of the foil for this time at temperature. The actual diffusion zone, as measured by maximum depth of carbide formation in the grain boundaries, was approximately 0.001 in., a value that is in close agreement with the calculated value.

The weight changes were quite small (<1 mg per foil), and the variation in the changes for the specimens may be a result of handling. However, there appeared to be a distinct trend toward greater weight loss at lower initial carbon concentration. This is in opposition to the expected order of weight change as a result of carbon transfer. The cause of this discrepancy has not yet been determined.

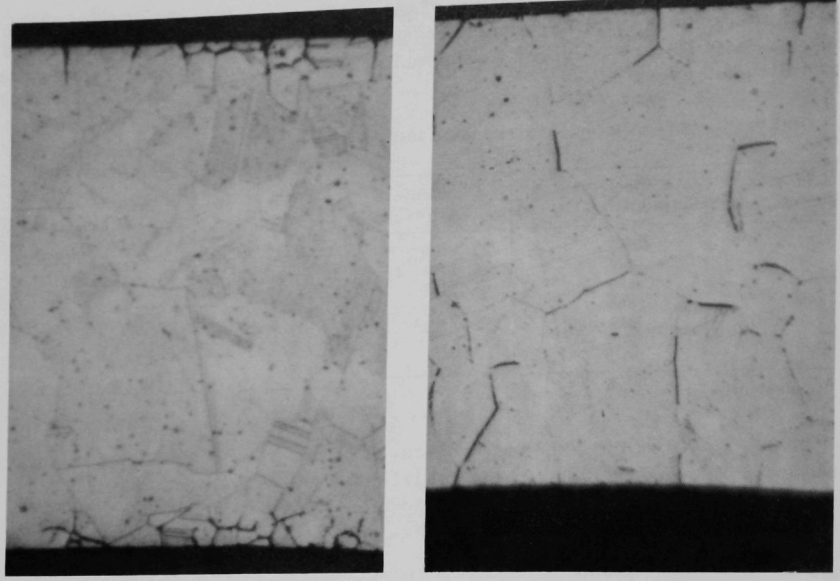

TC02 TC08

Samples Exposed to Primary Sodium

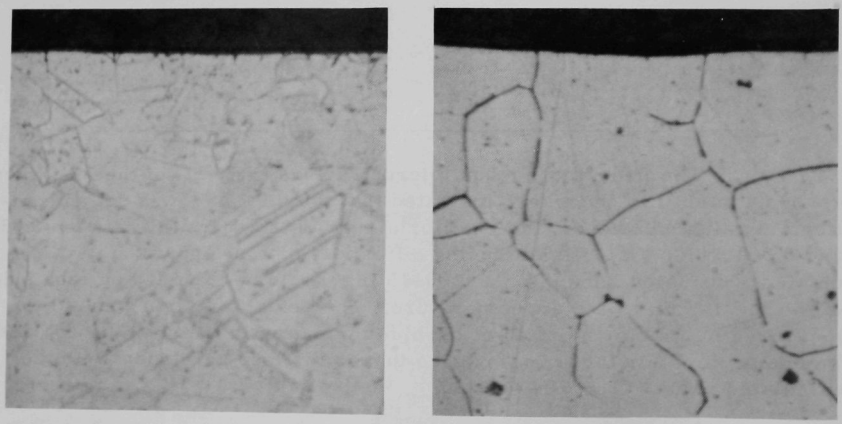

TC02 TC08

Control Samples in Helium-filled Capsule

Fig. 21. Microstructures of Types 304 (TC08) and 304L (TC02) Stainless Steel Equilibration Foils after Exposure in EBR-II (etched 45 sec in 5% oxalic acid). Mag. 400X.

3. Type 304 Stainless Steel Hexagonal Can from Subassembly XA08

Subassembly XA08 was in the primary tank of EBR-II for 43 months. Its exposure was equivalent to 278 full-power days at 45 MWt and 136 full-power days at 50 MWt. The average midplane fluence was 8.5×10^{22} nvt.

A section from the midplane of one flat of the hexagonal can enclosing the subassembly was examined optically and with the electron microprobe. Optical microscopy showed a sensitized structure, but no evidence of accelerated, localized, or other unexpected forms of corrosion. The electron-microprobe examination showed no selective dissolution of major alloying elements (iron, chromium, nickel, and manganese) from the surface. The small observed increase ($\sim\frac{1}{2}\%$) in chromium concentration in grain boundaries--both interior and close to the surface--is consistent with the observed sensitized structure, as is the carbon distribution. There was no evidence of carbon transfer to or from the surface.

The exposure temperature of the sample, calculated using the HECTIC code, was 423°C, a temperature that agrees well with a minimum temperature of approximately 425°C deduced from the observed metallographic structure.

4. Unclad Nickel and Chromium-plated Nickel

An in-reactor corrosion evaluation of nickel 200 and chromium-plated nickel was undertaken to provide assurance that unclad nickel could be used as a nuclear reflector for EBR-II. Two full-size subassemblies were prepared to provide gamma heating and sodium flow equivalent to that of the actual reflector design; each contained 30 carefully weighed nickel 200 rings, five of which were chromium-plated, stacked on a solid nickel bar. During the EBR-II exposure in row 7, the sodium temperature, with a flow of 1.2 gpm, varied from 700°F at the inlet to more than 900°F at the outlet.

The first of these subassemblies was evaluated[3] after an exposure of 58 days at power (equivalent to 2910 MWd). The second subassembly was in the reactor for 380 days (10,532 MWd) and accumulated a total fluence of $\sim 2 \times 10^{22}$ nvt at its centerline. The maximum sodium temperature, as indicated by melt-wire devices, was ~920°F.

Table IV shows the weight losses of the rings in the two subassemblies. The weight losses varied somewhat from specimen to specimen (probably because of variations in handling and cleaning), but all weight losses were low. The average weight loss of the four specimens at the top of the subassembly increased from 0.06 mg/cm^2 at 58 days to only

0.08 mg/cm^2 at 380 days. The maximum weight loss corresponds to somewhat less than 5 μin. of uniform nickel loss. Chromium plating reduced the weight loss.

TABLE IV. Weight Loss of Nickel 200 Rings[a] Exposed in EBR-II

Ring Position	Estimated Temperature, °F	Weight Loss, mg/cm^2	
		58 days	380 days
1 (Top)	920	0.061	0.094
2	920	0.065	0.087
3	920	0.049	0.057
4	920	0.062	0.079
5[b]	920	0.019	0.011
6	920	0.044	0.043
13[c]	920	0.050	0.052
14	890	-	0.051
15	860	-	0.044
16[b]	830	0.024	0.003
17	800	0.030	0.033

[a]Rings 2.16-in. OD x 2 in. long; 88 cm^2 exposed to sodium flowing at 1.2 gpm.
[b]Rings chromium-plated.
[c]Top of reactor core.

The nickel 200 in the core region of the second subassembly swelled noticeably as a result of its exposure to the fast flux. As a result, the subassembly bowed. Results of a detailed examination of the swelling will be reported elsewhere.[10]

C. Ex-reactor Tests Performed in Support of EBR-II

In many instances, it is possible to answer questions of material compatibility and provide increased confidence in proposed plant modifications by performing ex-reactor tests in sodium of a purity approximating that of EBR-II. Seven test programs of this type as described below, were performed during 1970.

1. Exposure of Irradiated Mixed-oxide Fuel to Sodium

A breach of the cladding of unencapsulated mixed-oxide fuel experiments currently in EBR-II could expose the fuel to primary sodium. Present plans tentatively call for removing a subassembly containing an experiment with such a breach to the EBR-II basket for temporary storage pending final disposition.

No experimental information was available regarding the extent and type of reaction between irradiated mixed-oxide fuel and relatively cool (~700°F) sodium. Accordingly, a limited program was initiated to study the extent of this reaction as a function of fuel composition, method of fabrication, and burnup. The only temperature used was 700°F; the index of extent of reaction was swelling and/or distortion of the fuel element. Such dimensional changes could, in turn, distort the subassembly, thereby causing handling problems and possibly damage of the EBR-II storage basket.

The experiments were done in an alpha-gamma cave, using a compact (2 x 2 x 0.8-ft) package test facility incorporating a test chamber, oxygen reservoir (cold trap), electromagnetic pump, and flowmeter. Samples were deliberately defected fuel elements that had been irradiated in EBR-II.

The loop was constructed, filled with sodium, and operated initially outside the cave. Several grams of sodium oxide were transferred into the cold trap. With this oxide in the trap, the oxygen in the sodium was controlled by setting the temperature of the trap. Analyses of the sodium by the distillation method gave values of 2 ppm oxygen when the cold trap was operated at 298°F and 7 ppm at 374°F. These analytical results agreed reasonably with those predicted from the solubility of sodium oxide[11] at the cold-trap temperatures. The solubility data were then used to select an operating range for the cold trap (250 ± 5°F) at which the oxygen level would be equivalent to that in EBR-II primary sodium (~1 ppm). Sodium flowed past the specimens at about 1 fpm.

The specimens were approximately 2-in.-long sections of the fuel elements with end caps. Each sample had an axial defect through the cladding and penetrating into the fuel. The defect was made by an abrasive wheel with a 15-mil-wide face.

Table V describes the samples. Tables VI-VIII give the results of exposure to 700°F sodium. Diameter measurements were made at several locations along the length of each sample. Appreciable changes in diameter

TABLE V. Characteristics of Defected Samples from Helium-bonded Fuel Elements Used for Studying Effects of Exposure of UO_2-20 wt % PuO_2 Fuel to Sodium

Element	Subassembly	Burnup, at. %	Fabricator	Element Diameter, in.	Cladding Material and (thickness in inches)	Method of Fabricating Fuel	O/M Ratio	% Theoretical Density		Defect Dimensions, in.[a]	
								Pellet	Smear	Length at Surface	Depth into Fuel
007	X040A	5.8	ANL	0.292	Type 304SS (0.020)	Coprecipitation	1.98	79.4	76.5	0.80	0.020
C15 (Top)	X012	9.6	NUMEC	0.262	Type 316SS (0.015)	Mechanical mixing	2.00	84[b]	82.4	0.83	0.028
C15 (Bottom)	X012	9.6	NUMEC	0.262	Type 316SS (0.015)	Coprecipitation	1.99	84[b]	83.0	0.66	0.013

[a]Defect made by 0.015-in.-wide x 4-in.-OD abrasive wheel.
[b]Nominal.

TABLE VI. Effect of Sodium Exposure at 700°F on Defected Sample from Fuel Element 007

Elapsed Time, days	Cumulative Diameter Change, mils		Cumulative Increase in Length, mils	Cumulative Weight Gain,[a] mg
	Normal to Defect	Plane of Defect		
2.0	+0.9	+1.3	1	167
6.6	+1.7	+2.1	2	194
15.2	+1.9	+2.1	2	289
28.8	+2.3	+2.2	2	273

[a]The weight gain is presumably due to sodium-logging. The maximum takeup of sodium is calculated to be 344 mg assuming that sodium fills the annular space around the pellet and has access to all porosity in the pellet.

TABLE VII. Effect of Sodium Exposure at 700°F on Defected Sample from Top of Fuel Element C15

Elapsed Time, days	Cumulative Diameter Change, mils		Cumulative Increase in Length,[a] mils	Cumulative Weight Gain,[b] mg
	Normal to Defect	Plane of Defect		
2.7	+2.9	+6.5	8.5	156
5.3	+4.3	+3.5	8.9	204
12.0	+4.1	+6.0	9.5	188
15.7	+4.6	+5.4	10.1	-
22.7	+4.4	+4.3	13.9	179
37.4	+2.3	+4.3	9.7	174

[a]Loose end caps are believed responsible for these large increases.
[b]Maximum sodium takeup based on same assumption used for element 007 is 226 mg.

TABLE VIII. Effect of Sodium Exposure at 700°F on Defected Sample from Bottom of Fuel Element C15

Elapsed Time, days	Cumulative Diameter Change, mils		Cumulative Increase in Length, mils	Cumulative Weight Gain,[a] mg
	Normal to Defect	Plane of Defect		
3.8	+2.4	+2.1	3.3	-
10.8	+2.2	+2.7	0.6	194
25.5	+1.8	-1.3	5.3	191

[a]Maximum sodium takeup based on same assumption as for element 007 is 213 mg.

were observed only at the midlength of the defect slit, so only those values are reported in the tables. Element C15 had marked ovality due to distortion caused by spacer wire. Because of this, slight rotational errors in placing C15 in the micrometer fixture caused relatively large changes in

the measured diameter. Thus, the diameter changes reported in Table VII show more scatter than those reported for fuel element 007 (see Table VI).

Visual examination of the samples under low magnification (up to ~10X) revealed no distortion or other gross changes. The cladding of the C15 samples had moved slightly away from the fuel, producing a "ledge" effect visible in the defect slit. This was noted after the first inspection, but did not change during subsequent exposure.

The method of grinding the defect slit produced a region of cladding at the end of the defects varying in thickness from essentially zero to full cladding thickness. Cracks became visible in the thinned regions of the cladding for the C15 samples after the first period of exposure, but did not propagate into the region of full cladding thickness (i.e., beyond the defect) during subsequent exposure.

The sample from element 007 was in the initial stages of metallographical examination at the time this report was being prepared. Inspection of several cross sections indicated that the central void (~0.092 in. in diameter) was completely filled with sodium. Figure 22 shows a cross section of the sample through the midlength of the defect. The relatively large void areas are not unique to this sample, but have been observed in the structure of other elements examined after irradiation. The depth of the defect is approximately the same as that before exposure, and the examinations to date have revealed no discernible effects of the sodium exposure. Microprobe analysis will be attempted to determine if any products of reaction of sodium and fuel were produced.

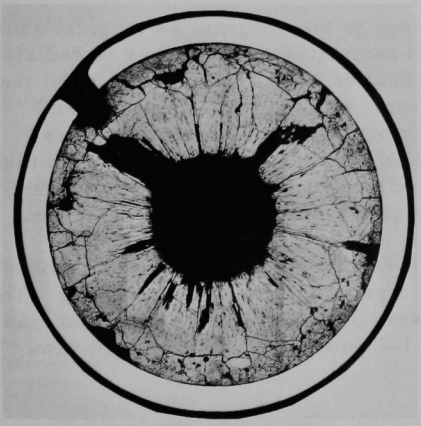

Fig. 22. Transverse Section of Defected Sample from Fuel Element 007 after Exposure to 700°F Sodium for 28.8 days. Mag. 9.75X. Neg. No. MSD-1432B.

The results to date indicate that reactor safety would not be compromised if failed mixed-oxide elements were stored in the storage basket for periods up to at least a month. Moreover, the samples did not appear to be changed sufficiently to affect evaluation by the experimenter. However, the presence of approximately 1.3 g of sodium in the central void of a 14-in.-long fuel element could lead to complications in the cleaning procedure. Therefore, after the 25.5-day exposure of the bottom section of C15, the sample was exposed to moist nitrogen for 1 day and

then to moist air for about 1 week. No gross effects have been observed on sample dimensions, but some fuel leached out in the initial moist-nitrogen treatment.

2. Experience with Corrosion of Free-machining Stainless Steels and Other Materials by Sodium

Machining costs would be reduced appreciably if Type 304 stainless steel were replaced with a free-machining and/or lower-cost grade of stainless in a variety of relatively complicated components of expendable core hardware for EBR-II. In addition, designers would have more flexibility if these alternative materials were acceptable. Therefore, a screening program was undertaken to determine if any of these materials might be acceptable.

The primary alternative materials considered were Types 201, 302, and 303 stainless steels. (The last would not be used for any fusion-welded component.) Type 304 stainless steel was included in the program as a basis for comparison.

Other materials were included in the program as original samples were removed for metallographic examination. The alloys tested also included: samples from a documented heat of Type 316 stainless steel that had been set aside for a material program; some developmental nickel alloys (with attractive high-temperature properties) furnished by International Nickel Company; and Type 304LN stainless steel, a relatively high-nitrogen (0.14% N), low-carbon (0.016% C) modification of Type 304 developed by U.S. Steel for increased resistance to intergranular penetration.

The samples, in the form of rectangular sheets, were exposed in a flowing-sodium loop equipped with a regenerative heat exchanger. The temperatures in the hot and cold legs were 1050 and 700°F. The cold trap was maintained at 257°F (equivalent to 1-2 ppm oxygen). Maximum flow rate was approximately 6 fps.

Table IX summarizes the weight-change data obtained. The weight changes for non-sulfur-containing Types 301, 304, 304LN, and 316 stainless steels were comparable. The free-machining, sulfur-containing Types 203EZ, 303, and 303CMC stainless steels lost appreciably more weight than those alloys that did not contain sulfur. The small size of the available samples of Type 201 stainless steel reduced somewhat the accuracy of the measurements for this material. The nickel-base alloys appeared to be suitable for use in sodium at these temperatures.

Metallographic examination and the weight-change data both indicated that the sulfur-bearing materials were not acceptable for use in a sodium environment. Metallographic examination showed that the sodium

TABLE IX. Weight Changes of Materials Exposed in Sodium

Material	Sodium Temp, °F	Sodium Velocity, fps	Weight Change, in mg/cm², after ... 34 days	35 days	69 days	77 days	111 days	146 days
201 SS	700	6		+0.037	-0.037			+0.11
	700	6		+0.037	-0.074			+0.074
	700	3		+0.074				
	1050	6		-0.15	-0.26			-0.33
	1050	6		-0.074	-0.18			-0.29
	1050	3		-0.037				
203EZ SS[a]	700	3	-0.10					
	700	3	-0.10					
	1050	3	-0.38					
	1050	3	-0.38					
301 SS	700	6		0.00	-0.027			+0.04
	700	6		+0.014	-0.014			+0.04
	700	3		+0.014				
	1050	6		-0.069	-0.14			-0.19
	1050	6		-0.082	-0.12			-0.15
	1050	3		-0.041				
303 SS	700	6		-0.064	-0.091			
	700	6		-0.064	-0.10			
	700	3		-0.073				
	1050	6		-0.46	-0.51			
	1050	6		-0.45	-0.51			
	1050	3		-0.48				
303CMC SS[b]	700	3	-0.15					
	700	3	-0.13					
	1050	3	-0.27					
	1050	3	-0.29					
304 SS	700	6		-0.0068[c]	-0.014[c]			+0.014[c]
	700	3		0.00	-0.028			-0.041
	1050	6		-0.068	-0.12			-0.17
	1050	3		-0.062	-0.090			-0.12
304LN SS	700	6		+0.022	-0.022			+0.033
	700	3		+0.022	-0.011			+0.019
	1050	6		-0.076	-0.13			-0.18
	1050	3		-0.065	-0.098			-0.14
316 SS	700	6				+0.024		
	700	3				+0.037		
	1050	6				-0.073		
	1050	3				-0.073		
INCO Alloy[d] (Microduplex[e])	700	3				+0.041		
	700	3				+0.028		
	1050	3				-0.19		
	1050	3				-0.11		
INCO Alloy[d] (Annealed[f])	700	3	-0.060				+0.060	
	1050	3	-0.060				-0.15	
INCO Alloy[g] (Microduplex[e])	700	3				+0.014		
	700	3				+0.028		
	1050	3				-0.055		
	1050	3				-0.056		
INCO Alloy[g] (Annealed[f])	700	3	-0.030				+0.030	
	1050	3	-0.059				-0.089	

[a]Allegheny-Ludlum alloy with nominal composition 17% Cr, 6% Ni, 6% Mn, 2% Cu, 0.3% S, 0.03% P, 0.05% C, balance Fe.

[b]Armco alloy with nominal composition 17-19% Cr, 8-10% Ni, 2% Mn (max), 0.6% Mo (max), 1% Si (max), 0.2% P (max), 0.15% C (max), 0.15% S (min), balance Fe.

[c]First (leading) sample exposed to sodium.

[d]International Nickel Co. alloy with nominal composition 44% Ni, 37% Cr, balance Fe.

[e]Coldworked 30%, heat-treated at 1800°F for 1 hr, then air-cooled.

[f]Heat-treated at 2300°F for 1 hr, water-quenched, reheat-treated at 1800°F for 2 hr, and then air-cooled.

[g]International Nickel Co. alloy with nominal composition 32% Ni, 32% Cr, balance Fe.

had dissolved the stringers of second-phase material (when stringers were interconnected) to depths up to 0.03 in. after 35 days of exposure (see Fig. 23). At the end of the test, penetration of the 0.065-in.-thick specimens was complete in the location of interconnected stringers. Only Type 203EZ stainless steel showed an unusual surface appearance, and only the sulfur-bearing materials showed the subsurface attack described above.

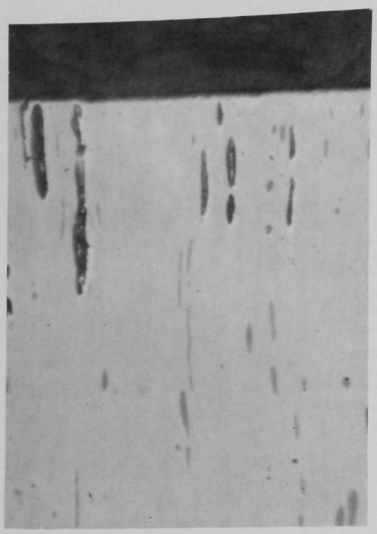

Fig. 23. Penetration of Type 303 Stainless Steel Exposed 35 days to 3-fps Flow of 700°F Sodium. Mag. 450X.

3. Behavior of Type 304 Stainless Steel in Sodium Containing 1500 ppm Tin

In July 1965, a sufficient quantity of bismuth-tin eutectic alloy found its way into the EBR-II tank to raise the tin concentration of the primary sodium to 15-20 ppm and the bismuth concentration to ~45 ppm. The action of the reactor purification system reduced the bismuth concentration to <2 ppm, but did not alter the tin concentration, because tin solubility at the cold-trap temperature is >1000 ppm. Type 304 stainless steel capsule bodies exposed in EBR-II during the period of high bismuth concentration showed no evidence of penetration of the stainless steel by either tin or bismuth. Optical metallography and the electron microprobe were both used for examining the capsule bodies.

It was apparent that a leak in the troughs of the fusible seals of the reactor could increase the tin concentration in primary coolant to much larger values; there is no known method of removing tin from the coolant. A series of ex-reactor capsule experiments was performed to provide advance information as to whether such a hypothetical incident would result in a destructive interaction of the sodium-tin solution with the stainless steel cladding of fuel elements.

Six capsules of Type 304 stainless steel were filled with sodium-tin solution, closed by electron-beam welding, and then exposed to high temperatures. Weighed Type 304L stainless steel tabs were included in each capsule. The capsules were protected by enclosure in a quartz vacuum ampule.

Table X gives the results of the exposures. No significant weight changes occurred. A loose deposit was noted on the inside of the capsules after dissolution of the sodium in alcohol, but too little was available for analysis. Chemical analysis of the alcohol used to dissolve the sodium-tin solution indicated incomplete recovery of the tin. The deposit observed was probably tin thrown out of solution in the sodium during the slow cooling of the capsule.

TABLE X. Capsule Experiments

Capsule No.	Temp, °F	Exposure Time, days	Tin Concentration, ppm	Description of 304L Sample Surface	Weight Change, mg/cm^2
SN1	1200	7	1460	Brown film, wiped off	-0.21
SN2	1020	30	1470	Brown film, remained on	+0.07
SN3	1020	7	1500	Brown film, remained on	+0.05
SN4	1200	30	0	Metallic, cloudy	+0.05
SN5[a]	1200	30	1480	Metallic, etched	+0.03
SN6	1200	30	1880	Metallic, cloudy	+0.05

[a]Inadvertently exposed to air during fabrication.

Sections of the capsule wall and the Type 304L stainless steel tab were examined in the as-polished condition and also after electroetching in 2 wt % oxalic acid. Comparison of a blank (no tin) specimen with the others showed no effect due to the presence of tin. A capsule (SN5) that had inadvertently been exposed to air briefly (during EB welding) showed evidence of very slight grain-boundary attack at the surface. This is a characteristic of the attack of sodium containing oxygen. A similar capsule that had not been exposed to air showed no grain-boundary attack.

Specimens SN2 and SN6 (each exposed 30 days) were examined with the electron microprobe. No evidence was found of tin penetration of the stainless steel.

4. Mechanical Strength of Brazed Joints Exposed to Sodium

The braze alloy used in certain fabrication steps for the instrumented subassemblies has a nominal composition of 20% chromium, 10% silicon, 3% iron, and the balance nickel. Stainless steel joints brazed with this alloy and also with alloys of similar composition have been shown to be resistant, in the sense of gross weight loss, to sodium at temperatures above those experienced by the instrumented subassembly.

However, metallographic studies and microprobe analyses by other investigators[12] indicated a loss of silicon and certain impurities to the sodium. No information was available on the effect of this material loss on the shear behavior of joints at 850°F. A relatively short test was completed which provided information in the temperature range of interest to EBR-II.

Specimens were prepared from Type 304 stainless steel rod stock. Wafers, 3/16 in. thick, were machined from a 1-in.-OD bar, and a 31/64-in.-dia axial hole was drilled through each wafer. Plugs for the holes were machined from 1/2-in.-OD rod and individually fit to a diametral clearance of 0.0015-0.002 in. The plugs were then brazed into the holes using the same procedure as specified for the instrumented subassembly. The wafers were then trimmed to 1/8-in. thickness to eliminate the fillets, and one side of each was metallographically polished to reveal the braze area. The wafers were then exposed to vacuum or sodium. After the exposure, the polished surface was reexamined. Then, the brazed plug was forced out in shear by a punch and die in a compression-testing machine. Table XI gives the shear stresses observed.

TABLE XI. Mechanical Evaluation of Brazed Joints

Type of Sample	Max Shear Stress, kpsi
Solid bar stock--no plug (as prepared)	79.5 79.3
Brazed plug, as brazed	57.5 66.9 59.7
Brazed plug, vacuum heat-treated 2 months at 850°F	64.7 32.5 54.9
Brazed plug, exposed to sodium for 2 months at 850°F; cold trap at 300°F	59.2 63.0 32.5

There appeared to be no loss of joint shear strength attributable to sodium exposure. The low values obtained for one vacuum-exposed and one sodium-exposed sample were attributable to a poorer initial braze, as judged from examination of the shear surfaces.

Negligible weight changes (±0.0001 g) were recorded for the sodium-exposed samples. Microscopic examination of the braze area indicated that the plugs were not evenly centered in the hole and that most of the diametral clearance accumulated on one side of the plug. The braze in the center of this wider band was attacked slightly by the sodium (see Fig. 24). No sodium attack was noted in the low-clearance regions of the joint or the adjacent diffusion zone in the stainless steel (see Fig. 25). The sodium exposure also brought out surface scratches on the previously metallographically polished stainless steel surface, as can be seen in the figures.

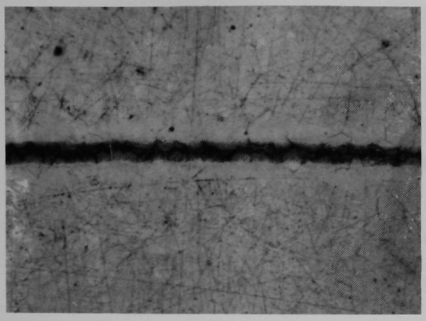

Fig. 24. Appearance of Wider Brazed Joint after Sodium Exposure. Mag. 135X.

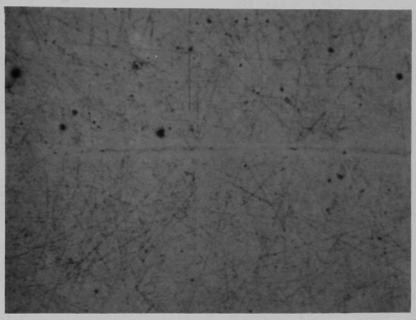

Fig. 25. Appearance of Low-clearance Region of Brazed Joint after Sodium Exposure. Mag. 135X.

5. Lifetests of Bellows Valves in Sodium

Two 2-in. and several 1-in. Belloseal bellows valves were purchased for use on the radioactive sodium chemistry loop (RSCL) to be added to the EBR-II plant. Subsequently, two similar 2-in. valves failed prematurely (see Sec. II.A.4) in ex-reactor testing. In our opinion, the travel of the bellows in the 2-in. valve was too long. The manufacturer, Wm. Powell, cooperated closely and refitted the 2-in. valves with tandem bellows, essentially cutting the travel per bellows to a conservative 20% (overall).

An an added precaution, one of the new tandem-bellows 2-in. valves was tested in 700°F, 30-psig sodium for 5000 complete cycles. The valve was then returned to the manufacturer for refitting with new bellows, and the used bellows were returned to us for our examination. No sign was found of sodium penetration of the bellows. No cracks or other imperfections were noted, and the microstructure of the bellows metal was free of concentrations of inclusions.

A similar lifetest was performed on a standard 1-in. Powell Belloseal valve. The valve also showed no sign of failure at 5000 complete cycles in sodium at 700°F and 30 psig. It still turned easily.

6. Engineering Testing of an Analytical Cold Trap

A prototype of an EBR-II analytical cold trap was designed by E. Filewicz of the EBR-II Project and fabricated under his direction. The trap provides a large surface area on which various compounds or elements may precipitate from the sodium stream throughout the range of temperatures in the trap.

The trap, shown in Fig. 26, is 2 in. in OD and about 46 in. long, and is designed to operate at a flow rate of 0.2 gpm (6 fpm) to achieve a

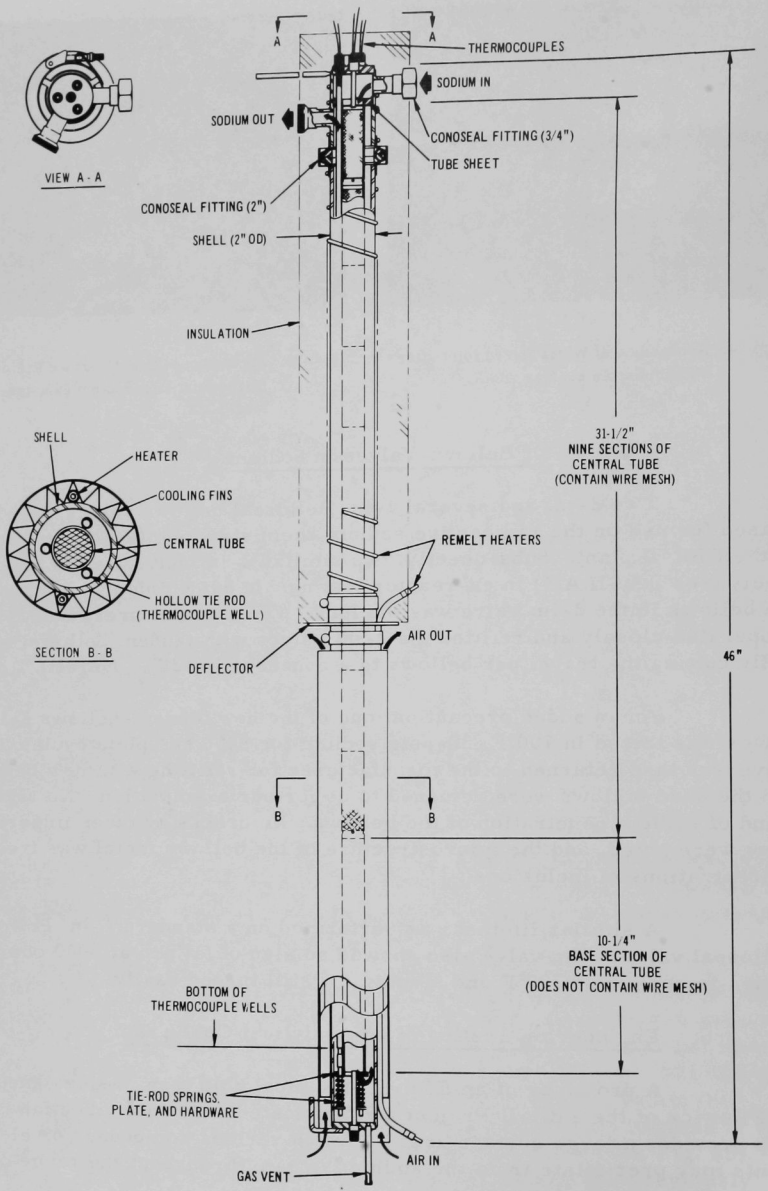

Fig. 26. Prototype of EBR-II Sodium Analytical Cold Trap

temperature of 220-700°F throughout its length. It is also designed so that the precipitates may be removed by nondestructive methods. The inlet and outlet connections and the housing closure have Conoseal flange fittings to allow easy removal and disassembly. The large surface areas for precipitation are provided by titanium wire mesh enclosed in nine $3\frac{1}{2}$-in.-long, 1-in.-OD sections of titanium tube. This sectionalized design simplifies disassembling of the trap and analysis of its contents. Titanium was selected because it is not of particular interest in the analysis of the trapped impurities. Though titanium is a getter of oxygen in sodium, the 700°F maximum operating temperature of the trap is well below the temperature at which gettering occurs.

Operation of the cold trap is based on the principle of the counterflow regenerative heat exchanger. Under design conditions, the sodium, at 700°F, enters through the top of the trap at about 0.2 gpm and flows down through the sectionalized central tube while being cooled by heat exchange with the sodium flowing countercurrently outside the tube. The temperature of the sodium at the bottom of the tube is as low as 220°F. From the bottom, the sodium flows upward through the annulus between the central tube and outer shell, being reheated along the way, and reaches a temperature as high as 660°F before leaving near the top of the trap. To establish and maintain the desired temperature relationships, air cooling is provided at the lower 18 in. of the trap. The upper 30 in. is insulated. The sections of the central tube are clamped together by three hollow, spring-loaded tie rods, which also serve as thermocouple wells, to prevent leakage of sodium between the central tube and the outer annulus and to allow differential longitudinal expansion between the Type 304 stainless steel shell and the titanium central tube. The thermocouple wells can be used for measuring temperatures at any point along the length of the trap.

The sections of the central tube may be removed after sodium has been drained from the outer annulus. To drain the annulus, the sodium-filled trap is removed from the circulating system, the inlet tube is capped, the trap is inverted, and the sodium is remelted and allowed to drain from the outer annulus only. (The central tube should not drain.) A connection has been provided at the bottom of the trap so that an inert gas can be introduced to assist the drainage. The sections of the central tube are removed by separating the 2-in. Conoseal fitting, removing the three pins, washers, and springs holding the tie rods, and removing the central tube. The sections of the central tube are separated by cutting through the frozen sodium between them with a sharp knife or blade.

The trap was inserted into a pumped-sodium system in which operating characteristics such as temperature gradient of the sodium, temperature control, and flow rates of cooling air were determined for sodium flow rates of 0.1, 0.2, and 0.3 gpm at a sodium inlet temperature of about 700°F and a minimum cold-trap temperature of 230°F. For an additional

test, copper was placed in the upstream line of the trap so that it would go into limited solution in the 700°F sodium stream and then precipitate out in the trap.

The trap performed satisfactorily in the operational tests and appeared to be relatively tolerant of normal variations in flow rates. Cooling air was supplied at a constant volume at the selected sodium flow rates to keep the temperature of the coldest sodium as constant as possible; about 2 cfm was required at a 0.2-gpm flow of sodium and about 10 cfm at a 0.3-gpm flow.

After the first few days, during which time the flow rate was varied, the trap operated at a constant rate of 0.2 gpm for the rest of the 25-day test. When the trap was disassembled, no sodium was in the inlet or the first few central sections. Apparently, at 1050°F, argon gas was absorbed by the sodium in the system and subsequently released and trapped in the central tube of the analytical cold trap upon cooling of the sodium stream. The released argon gas then rose to the top portion of the trap and displaced the sodium from that portion. This difficulty would be reduced or eliminated by operating the trap horizontally with the outlet upward. The potential for gas release would be lower in EBR-II, where the sodium/gas interface is at 700°F, than in our test system.

The copper that had been upstream of the trap lost 290 mg of its weight during the 25-day test. When the contents of the central tube sections were analyzed, two-thirds of the loss was found in these sections, which operated at 310-600°F. The colder portions of the trap were not packed with mesh, so analyses for copper recovery below 300°F could not be obtained. In future traps, the cold end will be sectioned and packed with mesh as are the other sections of the trap.

7. Effects of Nitrogen Contamination of Reactor Cover Gas

The argon cover gas for the EBR-II primary sodium system typically contains 0.25-0.50 vol % nitrogen as an impurity. During fuel handling, however, the nitrogen concentration may approach 1 vol %. When the reactor is operating, the sodium passes through the core, from which it leaves at temperatures as high as 1000°F at the 62.5-MWt power level. If nitrogen is transported from the cover gas into the sodium, nitriding of stainless steel components may result. Hence, a series of ex-reactor experiments was performed to evaluate the nitriding potential under conditions approximating those, except for neutron fluence, in the primary tank and in the core.

A preliminary experiment demonstrated that stainless steel could be nitrided in sodium. Type 304 stainless steel foils were exposed to 1020°F sodium under a nitrogen cover gas for 1 week, and similar foils

were exposed to the nitrogen atmosphere above the sodium. After exposure, metallographic examination of the foils revealed dense, continuous nitride layers extending to a depth of 0.4 mil into the foils exposed to the sodium and 0.7 mil into the foils from the cover-gas region. Figure 27 shows the nature of the nitride layer in a nitrogen-exposed foil.

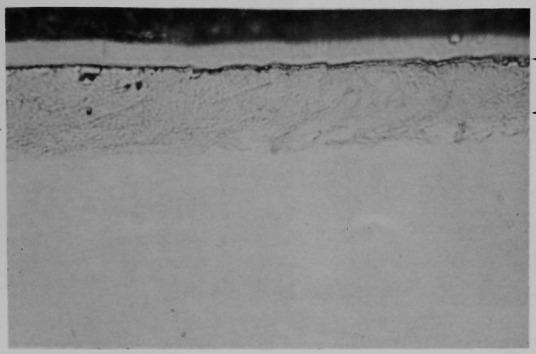

Fig. 27. Nitrided Layer on Type 304 Stainless Steel after One week in Nitrogen Gas Space above 1020°F Sodium (as polished). Mag. 900X.

To simulate the reactor cover gas more closely, commercially prepared gas mixtures of 0.1 and 1.0 vol % nitrogen in argon were used in subsequent tests. In these tests, Type 304 stainless steel foils were exposed to sodium at 1020 and 1200°F for 2 weeks under each of the two Ar-N_2 cover gases.

The exposed samples showed negligible weight gains (<0.01 mg/cm^2), and metallographic examination of transverse sections of the specimens revealed only slight nitriding at the grain boundaries of the surfaces exposed to sodium. Bulk chemical analysis of the foils indicated that the nitrogen content had not increased detectably above the 0.028 wt % in the original material.

The specimens for these tests had been electropolished before exposure. A comparison of the as-electropolished unexposed and sodium-exposed surfaces (Figs. 28 and 29) shows that nitrides formed both on the grain boundaries and on the grain faces having intimate contact with nitrogen-containing sodium.

A longer test involved exposing a 5-mil Type 304 stainless steel foil from a different heat to 700°F sodium under an Ar-1 vol % N_2 cover gas for 4 weeks. Under these conditions, only a slight amount of surface nitriding could be detected microscopically. Chemical analysis of the foil indicated no increase in nitrogen content above the level of 0.045 wt % in the as-received material. The material was not embrittled by the exposure.

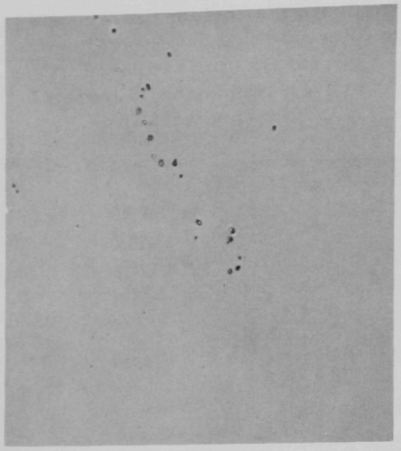

Fig. 28. As-electropolished Type 304 Stainless Steel Surface before Exposure to Hot Sodium under Ar-0.1 vol % N_2 Cover Gas. Mag. 900X.

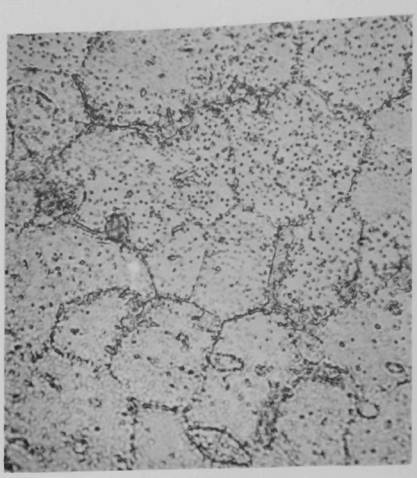

Fig. 29. Electropolished Type 304 Stainless Steel Surface Exposed to 1020°F Sodium under Ar-0.1 vol % N_2 Cover Gas. Mag. 900X.

In all the exposures cited in the preceding paragraphs, nitrogen was not replenished in the cover gas. The gas space above the sodium was pressurized to ~5 psia with the Ar-N_2 mixture at the start of the test, and the source was disconnected. To determine if nitrogen depletion of the cover gas may have been occurring, another test was conducted in which the Ar-1 vol % N_2 gas mixture flowed through the gas space at a low rate. Several Type 304 stainless steel foils were exposed to 700°F sodium and to the cover gas under these conditions for 96 days.

Chemical analyses of the foils showed no increase in nitrogen (or carbon) content, but the foils became embrittled as a result of their exposure. The reason for the degradation in mechanical properties is receiving continued study. The nitrogen content of the mixed gas is an unlikely cause.

No attempt was made to determine nitriding kinetics as a function of temperature and nitrogen activity under a wide variety of conditions. The results obtained did indicate, however, that only insignificant nitriding would be expected in EBR-II with its gas-interface temperature of 700°F. Examination of components exposed for long periods in the higher-temperature portions of the reactor tend to bear out this conclusion.

III. DISCUSSION

In general, the results of the materials-coolant investigations during 1970 tended to increase confidence in the LMFBR concept. The one

failure that caused a reactor shutdown was ascribed to a defect in one ply of a two-ply bellows. No evidence was found suggesting that the sodium environment was responsible for the initial defect, although the presence of sodium and air between the plies was blamed for the perforation of the second ply.

A common factor was noted in the failures of two other bellows, namely, the presence of inclusion stringers in the thin bellows wall. The experience gained in the testing of free-machining stainless steel suggested that sodium could actively leach out interconnecting sulfide-inclusion stringers and thereby cause tortuous leakage paths through the bellows wall. Use of radiography to detect the inclusion network proved useful for evaluating existing bellows, but stringent specifications should be adopted to ensure the use of stringer-free metal in the manufacture of new bellows for sodium service.

Another important factor reemphasized by our studies was the travel of the stem relative to the free length of the bellows. The literature indicated that a travel of 20% was conservative, but that any design requiring 30% or more travel should be critically examined. Experience with the 2-in. valves confirmed this general rule in that the premature mechanical failures of two bellows were obtained at 40% travel and no failure was sustained in a 5000-cycle test with 20% travel.

A. Materials Exposed to Primary Sodium

Examination of materials removed from the reactor indicated that their interaction with the sodium coolant was extremely small at the tank temperature of 700°F. At higher temperatures, slight dissolution of stainless steel, nickel, and chromium was noted.

For the first time, claddings of driver fuel elements that had operated at ~1080°F were available for examination. No evidence was found of selective attack by the sodium or of any microstructural changes that could be attributed to the reactor environment or the sodium-removal procedure. Similarly, examination of a hexagonal can exposed to $\sim 8.5 \times 10^{22}$ nvt uncovered no discernible effect of fluence upon the interaction of sodium and stainless steel.

Slow migration of carbon from Type 304 stainless steel ($C > 0.04\%$) and into Type 304L stainless steel was noted in an experiment designed to estimate the carburizing potential of EBR-II primary sodium. A uniform equilibrium microstructure was not reached, because the operating temperature was relatively low (870-890°F).

B. Ex-reactor Testing

A wide variety of testing was performed in support of EBR-II. Most of the tests indicated no hazard to operation of the reactor. The testing showed that sulfur-bearing stainless steels are not suitable for use in the reactor.

Experiments with irradiated mixed-oxide fuel were very encouraging for the LMFBR concept, since the interaction of the exposed fuel and sodium was minimal at the tank storage temperature (700°F). Swellings of the element normal to the defects were of the order of 2 mils after exposures ranging up to 37 days. No optically discernible changes were noted in the fuel.

ACKNOWLEDGMENTS

We gratefully acknowledge the assistance of many of the EBR-II personnel in obtaining the specimens and planning the tests described in this report.

We especially thank D. W. Cissel for his many helpful suggestions; D. E. Walker for the preparation of the braze specimen; J. R. Honekamp, L. A. Neimark, D. A. Donahue, and C. H. Gebo for their assistance with the testing of irradiated oxide fuel; E. M. Butler for his work with the microprobe; and D. J. Dorman for his assistance with operation of the sodium testing facilities.

REFERENCES

1. S. Greenberg, *The EBR-II Materials-surveillance Program: I. Program and Results of SURV-1*, ANL-7624 (Sept 1969).

2. S. Greenberg, R. V. Strain, and E. Ebersole, *The EBR-II Materials-surveillance Program: II. Results of SURV-2*, ANL-7682 (June 1970).

3. W. E. Ruther, T. D. Claar, S. Greenberg, and R. V. Strain, *Materials-Coolant Interactions in EBR-II*, ANL-7670 (Mar 1970).

4. Catalog R, *Syphon Seamless Metal Bellows and Bellows Assemblies*, p. 8, Robertshaw Company.

5. A. H. Barnes, F. A. Smith, and G. K. Whitham, "Experimental Breeder Reactor (CP-4)," *Reactor Engineering Division Quarterly Report: March 1, 1950 through May 31, 1950*, ANL-4481, pp. 3-8 (July 1, 1950).

6. P. Roy, G. P. Wozadlo, and F. A. Comprelli, "Mass Transport and Corrosion of Stainless Steels in Flowing Sodium Systems at 1300°F," *Proc. Int. Conf. on Sodium Technology and Large Fast Reactor Design, November 7-9, 1968*, ANL-7520, Part I, *Sessions on Sodium Technology*, pp. 131-142.

7. A. Thorley, R. Jackson, and J. Prescott, *The Effect of Different Carburizing Sources in Sodium on the Tensile Properties of Stainless Steel and Nimonic Alloys*, UKAEA TRG-2001(C), (1970).

8. C. C. Miles, *An Oxyacidic Flux Method for Determination of Carbon in Sodium*, Anal. Chem. *41*, 1041 (June 1969).

9. R. P. Agarwala, M. C. Naik, M. S. Anand, and A. R. Paul, *Diffusion of Carbon in Stainless Steels*, J. Nucl. Mat. *36*, pp. 41-47 (1970).

10. R. V. Strain and W. E. Ruther, *Results of Nickel-surveillance Tests in EBR-II* (ANL report to be published).

11. T. F. Kassner and D. L. Smith, *Calculations on the Kinetics of Oxygen Solution in Tantalum and Niobium in a Liquid-sodium Environment*, ANL-7335 (Sept 1967).

12. A. W. Thorley and C. Tyzack, "Corrosion Behaviour of Steels and Nickel Alloys in High-Temperature Sodium," *Alkali Metal Coolants*, pp. 97-118, IAEA, Vienna (1967).

B